Mechanical and Thermal Properties of Polyphenylene Sulfide/Multiwalled Carbon Nanotube Composites

Zhenyu Jiang, Peter Hornsby, Rauri McCool, Adrian Murphy

School of Mechanical and Aerospace Engineering, Queen's University Belfast, Belfast, BT9 5AH, United Kingdom

Received 18 January 2011; accepted 12 April 2011
DOI 10.1002/app.34669
Published online 31 August 2011 in Wiley Online Library (wileyonlinelibrary.com).

ABSTRACT: Polyphenylene sulfide (PPS)/multiwalled carbon nanotube (MWCNT) composites were prepared using a melt-blending procedure combining twin-screw extrusion with centrifugal premixing. A homogeneous dispersion of MWCNTs throughout the matrix was revealed by scanning electron microscopy for the nanocomposites with MWCNT contents ranging from 0.5 to 8.0 wt %. The mechanical properties of PPS were markedly enhanced by the incorporation of MWCNTs. Halpin-Tsai equations, modified with an efficiency factor, were used to model the elastic properties of the nanocomposites. The calculated modulus showed good agreement with the experimental data. The presence of the MWCNTs exhibited both promotion and retardation effects on the crystallization of PPS. The competition between these two effects results in an unusual change of the degree of crystallinity with increasing MWCNT content. © 2011 Wiley Periodicals, Inc. J Appl Polym Sci 123: 2676–2683, 2012

Key words: poly(phenylene sulfide); carbon nanotubes; nanocomposites; mechanical properties; crystallization

INTRODUCTION

Carbon nanotube (CNT)-reinforced polymer composites have gained increasing interest since the 1990s.[1,2] The exceptional mechanical, electrical, and thermal properties of CNTs, together with their nanoscale dimensions and high aspect ratio, make them superior additives for mechanical reinforcement of structural composites or fabrication of conductive polymers.[3] It has been extensively reported that the elastic modulus, strength, and fracture toughness of various polymers can be significantly enhanced by the incorporation of CNTs at modest loadings.[4] Furthermore, integration of CNTs into traditional fiber-reinforced composites have shown to achieve further improvement in mechanical performance, especially interlaminar and through-thickness properties.[5,6]

Polyphenylene sulfide (PPS) is a semicrystalline aromatic polymer which possesses excellent mechanical properties, good stability at elevated temperature, outstanding chemical resistance, and inherent flame retardancy. In addition to these advantages, the relatively low material cost and good processability make PPS a highly competitive engineering material among current high-performance thermoplastics. The global demand for PPS was estimated to maintain an annual growth rate of $\sim$ 10%.[7] However, high-end applications of PPS are still limited due to its inferior mechanical properties (strength and toughness) in comparison to the other commonly used aromatic thermoplastics, such as polyetheretherketone (PEEK) and polyetherimide (PEI). To overcome those deficiencies, considerable research effort has been dedicated to PPS-matrix composites. Modification of PPS with nanoparticles,[8–16] nanoclay,[17–19] and nanotubes[20–24] have undergone rapid development in recent years and showed remarkable reinforcing effects on the mechanical, thermal, and wear properties.

A few research work concerning CNT-reinforced PPS composites has been reported very recently. Addition of multiwalled carbon nanotubes (MWCNTs), via melt-blending[22–24] or direct powder-mixing followed by compression molding,[20,21] was found to significantly improve the mechanical properties of PPS. Yu et al.[22] achieved increases of 35 and 206% in Young's modulus and tensile strength respectively, by adding 7 wt % MWCNTs into PPS. Wu et al.[23] also observed that Young's modulus and tensile strength were increased by 86 and 209% in PPS with the same MWCNT loading. However, it was notable in those studies that the mechanical properties of the unfilled PPS were below the expected level. For instance, the tensile modulus and strength of unfilled PPS reported by the two aforementioned groups were only 1.4–1.8 GPa and 20–26 MPa respectively, far less than the ever known

Correspondence to: Z. Jiang (zhyjiang@ustc.edu).
Contract grant sponsor: Department for Employment and Learning, Northern Ireland ('Sustainable Transport' project under the 'Strengthening the All-Island Research Base' Programme).

TABLE I
Statistical Distribution of Nanotube Diameter For Nanocyl NC 7000

CNT diameter [nm]	5	6	7	8	9	10	11	12	13	14	15	17	18	19	20	22	23
Frequency [%]	1	5	10	3	14	16	14	15	6	4	4	2	1	1	2	1	1

Reproduced from Ref. 27.

values (i.e., 2.6–3.8 GPa and 65–86 MPa).[25,26] Even though the tensile strength of the PPS/MWCNT composites was greatly increased, it was still lower than that of commercially available unfilled PPS.

Contradictory observations related to thermal properties of PPS/MWCNT composites were also shown in the published work. It was found that the peak crystallization temperature (T_c) of PPS monotonically increased with the addition of MWCNTs.[23,24] However, another study demonstrated that T_c of PPS/MWNCT was 5–10°C lower than that of unfilled PPS.[22] One group reported an increase in peak melting temperature (T_m) caused by the presence of MWCNT,[23] whereas others observed that T_m of PPS/MWCNT composites exhibited a gradual decrease.[22,24] The existing inconsistencies necessitate the further investigations to achieve an unambiguous understanding of the properties of PPS/MWCNT composites.

This article addresses two issues. The first concerns the preparation of PPS/MWCNT composites. A processing strategy that combines melt-blending with premixing of PPS resin and CNTs in powder form is applied to achieve a homogeneous dispersion of MWCNTs within the PPS matrix. The second involves an exploration of the effects that MWCNTs impose on the mechanical and thermal properties of PPS. The fundamental role of nanotubes in the reinforcement mechanism is discussed according to experimental findings and theoretical analysis. The influence of MWCNTs on the crystallization and melting behavior of PPS was studied using differential scanning calorimetry (DSC).

EXPERIMENTAL

Materials

The matrix material was a commercial PPS product (Fortron 0214, Ticona) suitable for extrusion and injection molding, supplied in powder form with an average particle size of 300 μm.

Thin MWCNTs (NC 7000), produced via catalytic chemical vapor deposition, were provided by Nanocyl SA. The geometric features of this product were determined by Morcom et al.[27] using transmission electron microscopy (TEM) and scanning electron microscopy (SEM). Their measurement of 100 MWCNTs gave an average diameter and length of 10.4 nm and 0.7 μm, respectively, along with a distribution for CNT outside diameters ranging from 5 to 23 nm, as listed in Table I. On the basis of their study, physical parameters of NC 7000 MWCNTs can be calculated using the method proposed by Thostenson and Chou.[28] Assuming that the graphitic layers of the nanotube shell have the same density as fully dense graphite ($\rho_g = 2.25$ g/cm^3), the density of individual MWCNT (ρ_{CNT}) can be calculated by:

$$\rho_{CNT} = \frac{\rho_g(d^2 - d_i^2)}{d^2} \quad (1)$$

where d and d_i are outside and inside diameters of the nanotube, respectively. In this work, the value obtained from Ref. 27 were used, namely $\rho_{CNT} = 1.85$ g/cm^3. The effective modulus of nanotube (E_f) can be estimated according to the assumptions that the outer layer of the MWCNT carries nearly the entire load transferred from the matrix and the outer wall acts as an effective solid fiber, using

$$E_f = \frac{4t}{d} E_{CNT} \quad (2)$$

where t is the thickness of the outer layer (~ 0.34 nm),[28] and E_{CNT} represents the elastic modulus of the nanotube (~ 1.0 TPa).[29] eq. (2) is valid when (t/d) < 0.25.

Preparation of PPS/MWCNT composites

All materials were dried in an air circulation oven at 110°C for 6 h before processing. The PPS powders and MWCNTs were then premixed using a high-speed centrifugal mixer (Rondol Technology) at 3000 rpm for 30 s, as illustrated in Figure 1. The large agglomerates of nanotubes, with size beyond submillimeter level, were clearly visible to naked-eye before the premixing. This process effectively eliminated those agglomerates and achieved a uniform distribution of MWCNTS coated on the PPS powder. The mixtures were then melt-blended in a HAAKE twin-screw extruder (Rheomex PTW 16) equipped with 16 mm diameter corotating screws. The processing temperatures were maintained at 300, 310, and 290°C along the extruder barrel, and the screw speed held at 150 rpm. Five PPS/MWCNT compounds with CNT weight fractions of 0.5, 1.0, 2.0,

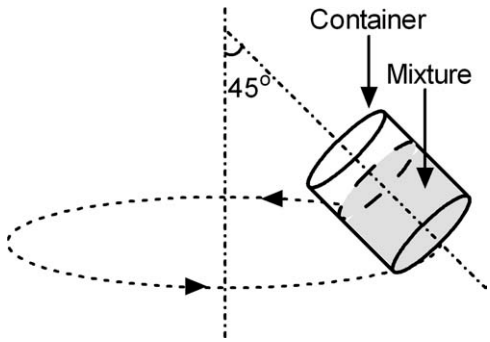

Figure 1 Illustration of centrifugal premixing.

4.0, and 8.0% were prepared in this study. Unfilled PPS was also processed though the same extrusion procedure as the control sample.

Mechanical test specimens were prepared on an Arburg Allrounder 320S 500-150 injection molding machine, with barrel temperature profile ranging from 290 to 320°C. The mold temperature was set at 70°C using a water circulation temperature controller.

Characterization and test

Morphological characterization of the PPS/MWCNT composites was conducted on a field emission environmental SEM (JEOL JSM-6500F) using an accelerating voltage of 5 kV.

The mechanical performance of the nanocomposites was evaluated through tensile and flexural tests undertaken on a universal tester (Instron 4411), following ASTM D 638 and D 790. In all tests, the distance traveled by the upper crosshead was used to calculate the breaking strain of the samples, which were out of the measurable range of the available extensometer.

DSC was conducted on a Perkin–Elmer DSC-6 to analyze the nonisothermal crystallization and melting behavior of PPS and its nanocomposites. Samples with a typical mass of $\sim$ 10 mg were sealed in aluminum pans and heated from 25 to 310°C, then held at this temperature for 5 min to eliminate thermal history present in the materials. The samples were then cooled and heated again in the same temperature range at a scanning rate of 5°C/min. The degree of crystallinity (χ_c) was calculated from the DSC data according to the following equation:

$$\chi_c = \frac{\Delta H}{\Delta H_f(1 - W_f)} \quad (3)$$

where W_f denotes the weight fraction of the MWCNTs. ΔH represents the enthalpy of fusion, and ΔH_f is the enthalpy of fusion for 100% crystalline PPS, taken as 112 J/g.[30] The property values obtained here represent an average of the results for tests run on two specimens.

RESULTS AND DISCUSSION

Dispersion of MWCNTs in PPS matrix

Figure 2 shows typical SEM micrographs of the cryo-fractured surface of PPS filled with 2.0 and 8.0 wt % MWCNTs. It can be seen in the photos taken at $\times$15,000 magnification that the MWCNTs are homogeneously distributed as individual nanotubes. The length of the nanotubes which partially expose on the fracture surface varied from about a hundred nanometers to one micron. The photos at $\times$35,000 magnification show that the MWCNTs are well embedded within the PPS matrix.

Mechanical properties of PPS/MWCNT composites

The mechanical properties of the PPS nanocomposites were improved markedly in comparison to unfilled PPS (Table II). The Young's modulus (E) and tensile strength were increased by 36 and 12% respectively, in PPS filled with 8 wt % MWCNT. It is interesting that the increase in mechanical properties of the PPS/MWCNT composites did not keep a constant proportion to the CNT loading, even though there was no evident deterioration of CNT dispersion at high CNT loadings according to Figure 2. As shown in Figure 3, a turning point appeared around 1–2 wt %, indicating that the nanotubes were less effective in reinforcement at higher CNT loadings. The reinforcement magnitude (dE/dV_f, where V_f is volume fraction of CNTs) of melt-processed MWCNT-reinforced thermoplastics was found to vary from $\sim$ 2.4 to $\sim$ 64 GPa.[4,31] In our study, dE/dV_f reached a high level ($\sim$ 60.5 GPa) at low CNT loading (0.5 wt %) but gradually fell to a modest level (15.8 GPa) when CNT content was above 1.0 wt %. This decrease in reinforcing efficiency will be considered in our modeling work, as discussed below. The breaking strain of PPS nanocomposites exhibited a monotonic decrease with increasing CNT content. With 8.0 wt % MWCNT it was reduced by 46% compared to that for unfilled PPS. These results may reflect the confining effect of MWCNTs on the movement of polymer chains at room temperature. An analogous enhancement was also found in the flexural properties. The flexural modulus and strength of PPS nanocomposites were increased by up to 20 and 14%, respectively.

The reinforcing effect of MWCNTs on the strength of polymers varied in a wide range in different work.[4,32,33] Incorporation of CNTs into high-performance thermoplastics was found to demonstrate less dramatic enhancement in strength than that

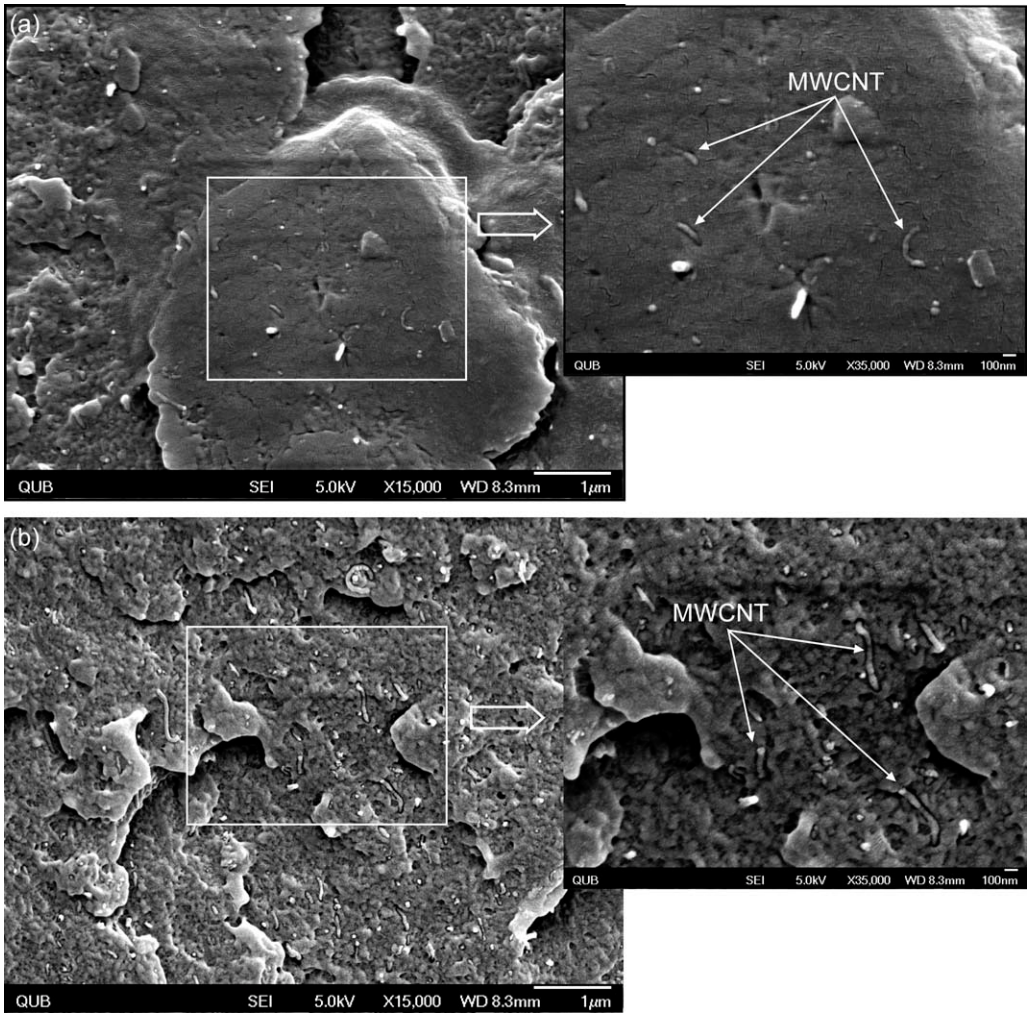

Figure 2 SEM micrographs of cryo-fractured surfaces of PPS with (a) 2.0 wt % MWCNT and (b) 8.0 wt % MWCNT.

expected by theory or that observed in the nanocomposites based on thermosets and common thermoplastics. Only a 12–14% increase in tensile and flexural strength was observed in our work. The addition of MWCNT into PEEK was also reported to yield an insignificant increase, up to 5.7% and 7.5%, in tensile and flexural strength, respectively.[34] The reason for this still remains unclear, and may relate to an insufficient load transferring between the CNTs and host polymers.

Stress transfer from polymer matrix to nanotubes is considered as a main reinforcement mechanism in CNT-reinforced composites. Therefore the elastic properties of CNT-reinforced polymers can be modeled using composite theory developed for short fiber-reinforced polymers,[4,28] which defines the modulus of the composite as a function of the elastic properties of the fibers and matrix, together with the aspect ratio of the fibers and their alignment relative to the applied stress. For randomly aligned

TABLE II
Mechanical Properties of PPS/MWCNT Composites

MWCNT content (wt %)	Young's modulus (GPa)	Tensile strength (MPa)	Breaking strain (%)	Flexural modulus (GPa)	Flexural strength (MPa)
0	3.10 ± 0.04	75.75 ± 0.77	5.97 ± 0.68	3.48 ± 0.07	88.15 ± 1.20
0.5	3.33 ± 0.03	77.13 ± 0.93	5.44 ± 0.30	3.32 ± 0.05	88.07 ± 3.54
1	3.41 ± 0.01	79.73 ± 0.50	5.01 ± 0.70	3.56 ± 0.06	88.52 ± 1.29
2	3.50 ± 0.06	82.50 ± 1.64	3.69 ± 0.60	3.58 ± 0.09	92.36 ± 2.76
4	3.77 ± 0.02	83.54 ± 0.87	3.57 ± 0.46	3.72 ± 0.07	94.00 ± 1.87
8	4.23 ± 0.04	85.03 ± 1.40	3.23 ± 0.23	4.18 ± 0.15	100.11 ± 1.76

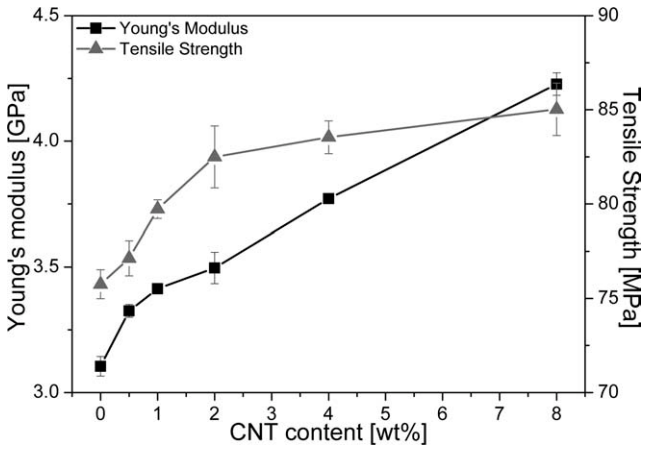

Figure 3 Mechanical properties of PPS/MWCNT composites.

MWCNTs, the elastic modulus of the composite (E_c) can be predicted by the Halpin-Tsai equation[4,35]:

$$\frac{E_c}{E_m} = \frac{3}{8}\left(\frac{1+\zeta\eta_L V_f}{1-\eta_L V_f}\right) + \frac{5}{8}\left(\frac{1+2\zeta\eta_T V_f}{1-\eta_T V_f}\right) \quad (4)$$

$$\zeta = \frac{2l}{d} \quad (5)$$

$$\eta_L = \frac{E_f/E_m - 1}{E_f/E_m + \zeta} \quad (6)$$

$$\eta_T = \frac{E_f/E_m - 1}{E_f/E_m + 2} \quad (7)$$

where E_m is the elastic modulus of polymer matrix, and l is the average length of nanotubes. ζ is a parameter depending on the geometry and boundary conditions of the reinforcements. η_L and η_T are the efficiency factors of reinforcements along and perpendicular to the tensile direction, respectively. V_f represents the volume fraction of the nanotubes, which can be calculated from

$$V_f = \frac{1}{1 + \frac{\rho_{CNT}}{\rho_m}\left(\frac{1}{W_f} - 1\right)} \quad (8)$$

where ρ_m is the density of polymer matrix (for PPS, $\rho_m = 1.35$ g/cm^3).[36]

The elastic modulus of each PPS nanocomposite predicted using eqs. (2), (4–8) and the distribution of nanotube diameters (Table I) exhibited a good agreement with the measured results at low CNT loadings (below 1.0 wt %), as shown in Figure 4. However, the predicted modulus began to exceed the experimental data at CNT loadings higher than 1.0 wt %. And the divergence between the predicted and measured values became larger with increasing CNT content. This overestimation was also reported for high-density polyethylene-reinforced with Nanocyl MWCNTs of various types (including NC 7000).[27] It is intriguing since the Halpin-Tsai equation is usually known to fit the real modulus very well at low CNT loadings but to give underestimated results at high CNT loadings.[4] Therefore, the decrease in reinforcing efficiency of MWCNTs at high CNT loadings should be taken into account in the model. Hence an efficiency factor [$F(V_f)$] as a function of CNT volume fraction was introduced to modify the Halpin-Tsai equation:

$$E_c = F(V_f)\left[\frac{3}{8}\left(\frac{1+\zeta\eta_L V_f}{1-\eta_L V_f}\right) + \frac{5}{8}\left(\frac{1+2\zeta\eta_T V_f}{1-\eta_T V_f}\right)\right]E_m \quad (9)$$

The analysis of data revealed that the difference between the moduli measured in experiments and predicted by original Halpin-Tsai model grew in a quasi-linear way with the increasing CNT loading. Therefore, $F(V_f)$ was assumed to be a linear function of V_f, and expressed as

$$F(V_f) = 1 + \alpha V_f \quad (10)$$

where α represents a decay factor, which can be determined by linear fitting of the difference between the measured modulus and the original Halpin-Tsai model predicted modulus, i.e., $\alpha = -4.46$. The negative value of α indicates that the reinforcing efficiency of MWCNTs decays with the increasing CNT loadings. According to eq. (10), it can be estimated that 22.4 vol % (28.3 wt %) is likely a critical loading for PPS filled with NC 7000 MWCNTs. The addition of NC 7000 MWCNTs over this level may result in deterioration of the elastic modulus of PPS nanocomposites.

The modulus predicted using the modified model compares well with the experimental data, as shown in Figure 4. To verify this model further, we applied

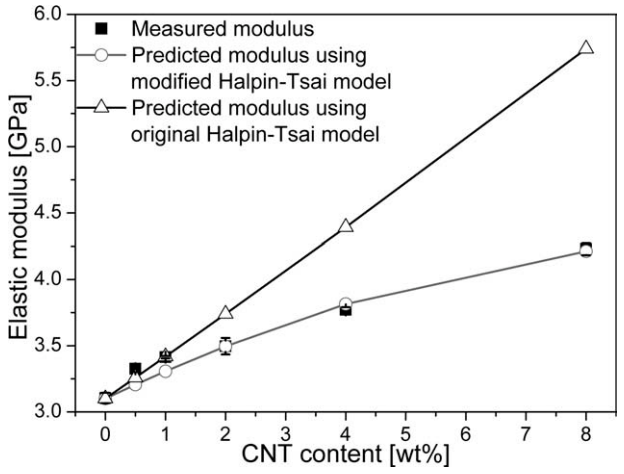

Figure 4 Prediction of elastic modulus of PPS/MWCNT composites using Halpin-Tsai equations.

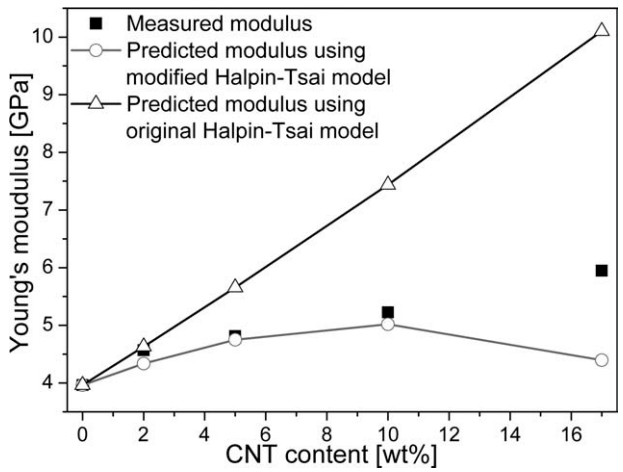

Figure 5 Prediction of elastic modulus of PEEK/MWCNT composites using Halpin-Tsai equations. The experimental values were obtained from Ref. [37]

it to the published experimental results for PEEK nanocomposites filled with NC 7000 MWCNTs, prepared by twin-screw extrusion.[37] The modulus calculated using eqs. (9) and (10) was shown in Figure 5, in comparison with the modulus measured by tensile test and predicted by original Halpin-Tsai model. It can be seen that the modulus predicted by our model was close to the experimental data at the CNT loadings ranging from 2 to 10 wt %, whereas the original Halpin-Tsai model still made overestimation. However, both the original and modified Halpin-Tsai models gave a considerable deviation from the experimental result at a very high CNT loading (17 wt %), indicating that other factors likely have an influencing role in the reinforcement mechanism at that loading level.

Crystallization and melt behavior of PPS/MWCNT composites

The addition of MWCNTs demonstrated an unconventional effect on the crystallization of PPS. Figure 6a shows the typical cooling DSC thermograms of PPS/MWCNT composites. The peak crystallization temperature (T_c) of PPS and its nanocomposites was around 253°C. Between the CNT content of 0.5 and 4.0 wt %, the onset crystallization temperature ($T_{c\text{-onset}}$) remained at the same level (about 269°C). But a distinct shift (about 10°C) of the ending temperature ($T_{c\text{-end}}$) towards the lower end was observed in the nanocomposites (as listed in Table III), indicative of a slowed crystallization process. According to the DSC data, the time that the PPS nanocomposites took for complete crystallization was about 100 s longer than the unfilled PPS. Similar observations were also reported in MWCNT-filled Nylon 66[38] and single-walled CNT-filled PEEK.[39] In those studies, the addition of CNTs (up to 2 wt %) did not change $T_{c\text{-onset}}$ for the nanocomposites, but slowed down crystallization process, leading to a lower T_c or $T_{c\text{-end}}$. The crystallization of PPS with 8.0 wt % MWCNTs started slightly earlier (at 271°C), and lasted as long as the other nanocomposites. A discernible shoulder can be seen on the left side of the crystallization peak (around 232°C) when the CNT content exceeds 4.0 wt %. The degree of crystallinity of the nanocomposites exhibited an unusual tendency. The χ_c was found to reach its peak value at CNT loading of 0.5 wt %, 12% higher than that for unfilled PPS. However, increases in CNT content gave no further rise but instead a small reduction in the crystallinity of the PPS nanocomposites, as compared with the highest level.

Carbon nanotubes have been extensively reported to act as nucleating agents and to accelerate the crystallization rate.[40–42] However, our observations show that MWCNTs have a dual effect on the crystallization of PPS. In addition to promoting nucleation, MWCNTs can also impose a confinement on the movement of polymer chains and hamper crystal growth.[38,39,43] These two effects competed against each other during the crystallization process, leading

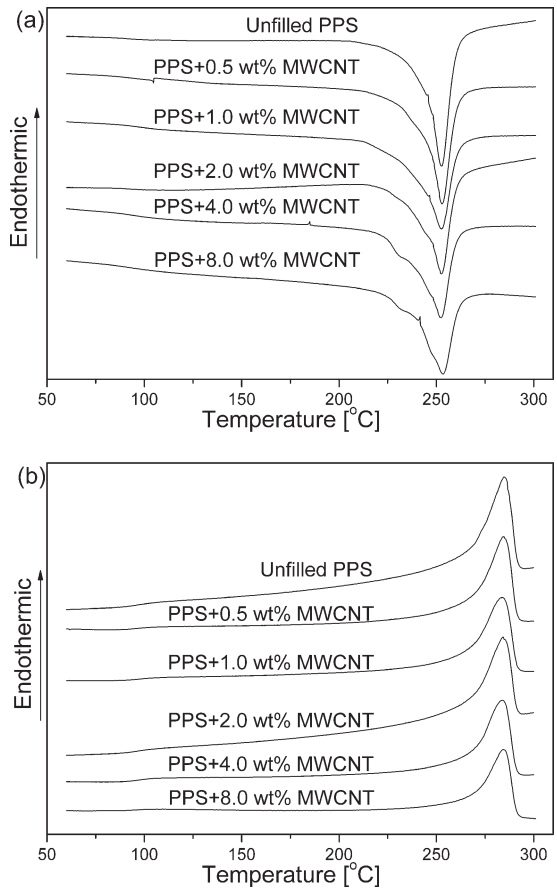

Figure 6 Nonisothermal DSC thermograms of PPS/MWCNT composites at (a) 1st cooling stage and (b) 2nd heating stage.

TABLE III
Crystallization and Melting Data of PPS/MWCNT Composites Obtained Through DSC

MWCNT content (wt %)	T_c (°C)	$T_{c\text{-onset}}$ (°C)	$T_{c\text{-end}}$ (°C)	χ_c (%)	T_m (°C)	$T_{m\text{-onset}}$ (°C)	$T_{m\text{-end}}$ (°C)
0	252.75 ± 0.08	268.37 ± 0.75	226.58 ± 0.09	32.76 ± 2.49	285.03 ± 0.50	252.30 ± 0.35	295.59 ± 0.86
0.5	252.69 ± 0.37	269.18 ± 2.09	216.38 ± 0.94	36.76 ± 1.78	284.69 ± 0.65	251.61 ± 0.68	295.38 ± 1.17
1	252.62 ± 0.11	268.38 ± 0.95	216.72 ± 0.66	35.48 ± 1.22	284.05 ± 0.93	250.27 ± 0.27	295.97 ± 2.01
2	252.21 ± 0.46	268.17 ± 1.99	217.51 ± 0.11	35.00 ± 0.72	284.41 ± 0.44	251.50 ± 1.10	295.73 ± 0.37
4	252.21 ± 0.28	269.71 ± 2.26	216.91 ± 0.37	36.09 ± 1.26	284.25 ± 0.35	251.28 ± 0.47	295.51 ± 1.03
8	252.95 ± 0.75	271.18 ± 1.12	219.31 ± 0.76	35.37 ± 0.12	284.31 ± 0.24	252.50 ± 0.44	295.72 ± 0.48

to a dependency of the crystallization behavior of PPS on MWCNT loading. On one hand, the additional sites present on the surface of CNTs can promote the formation of more crystalline structure and make the crystallization start earlier at high CNT loading (e.g., 8 wt %). On the other hand, the organization of polymer chains into ordered crystalline arrangements was suppressed by the MWCNT network within the polymer matrix, hence a slowed crystallization process was observed. The promotion effect has the initiative in this competition at low CNT loadings (e.g., 0.5 wt %), leading to a significant increase in degree of crystallinity. Nevertheless, the confinement effect gradually takes a dominant role with increasing CNT loading, finally resulting in a slight decrease in crystallinity.

The melting behavior of PPS nanocomposites was almost unchanged with the presence of MWCNTs, as shown in the DSC thermograms measured during the second heating stage [Fig. 6(b)]. In all six systems, the peak melting temperature (T_m) was about 284°C, and both the onset and end points remained similar (Table III).

CONCLUSIONS

This work documents the preparation of PPS/MWCNT composites through a controlled melt-blending procedure. An efficient dispersion of the nanotubes in PPS matrix with loadings in the range from 0.5 to 8.0 wt % was achieved by combining twin-screw extrusion with high-speed centrifugal premixing.

MWCNTs showed a marked reinforcing effect on the mechanical properties of PPS. Increases up to 36 and 14% were observed in modulus and strength, respectively. However, the magnitude of this effect was less than expected, considering the superior mechanical properties of CNTs. Furthermore, the reinforcing efficiency of MWCNT was found to decrease at high CNT loadings. On the basis of this observation, the Halpin-Tsai equation was modified to include an efficiency factor, which was linearly related to CNT volume fraction. This theoretical model was found to effectively predict the elastic modulus of MWCNT-reinforced high performance thermoplastics, including PPS and PEEK (using published experimental data), over a specified range of CNT loadings.

The incorporation of MWCNTs exhibited both promotion and retardation effects on the crystallization in PPS. The former, prevalent at low CNT contents, led to an increase in the degree of crystallinity, whereas the latter slowed down the crystallization process and resulted in less overall crystallinity at high CNT contents. These two competing roles yielded a dependency of crystallization behavior on CNT content, manifesting itself in an unusual change of the degree of crystallinity in PPS nanocomposites as function of CNT weight fraction. The melting behavior of PPS was nearly not affected by MWCNTs, which could be beneficial from an industrial point of view since no additional energy will be required in the further processing of PPS/MWCNT composites when thermoforming them into desired shapes or using them as matrix materials for fabrication of advanced fiber-reinforced composites.

The authors thank Mr J. Kissick, Dr. P. Hanna and Dr. S. McFarland at Queen's University Belfast for their kind assistance in twin-screw extrusion, injection molding and SEM characterization, respectively.

References

1. Thostenson, E. T.; Ren, Z.; Chou, T.-W. Compos Sci Technol 2001, 61, 1899.
2. Baughman, R. H.; Zakhidov, A. A.; de Heer, W. A. Science 2002, 297, 787.
3. Moniruzzaman, M.; Winey, K. I. Macromolecules 2006, 39, 5194.
4. Coleman, J. N.; Khan, U.; Blau, W. J.; Gun'ko, Y. K. Carbon 2006, 44, 1624.
5. Qian, H.; Greenhalgh, E. S.; Shaffer, M. S. P.; Bismarck, A. J Mater Chem 2010, 20, 4751.
6. Chou, T. W.; Gao, L.; Thostenson, E. T.; Zhang, Z.; Byun, J. H. Compos Sci Technol 2010, 70, 1.
7. Platt, D. K. Engineering and High Performance Plastics; Rapra Technology Ltd: Shawbury, 2003.
8. Schwartz, C. J.; Bahadur, S. Wear 2000, 237, 261.
9. Lu, D.; Yang, Y.; Zhuang, G.; Zhang, Y.; Li, B. Macromol Chem Phys 2001, 202, 734.
10. Lu, D.; Mai, Y.-W.; Li, R. K. Y.; Ye, L. Macromol Mater Eng 2003, 288, 693.
11. Bahadur, S.; Sunkara, C. Wear 2005, 258, 1411.

12. Cho, M. H.; Bahadur, S.; Pogosian, A. K. Tribol Int 2006, 39, 249.
13. Lu, D.; Pan, S. Polym Eng Sci 2006, 46, 820.
14. Wang, X.; Tong, W.; Li, W.; Huang, H.; Yang, J.; Li, G. Polym Bull 2006, 57, 953.
15. Naffakh, M.; Marco, C.; Gomez, M. A.; Jimenez, I. J Phys Chem B 2008, 112, 14819.
16. Naffakh, M.; Marco, C.; Gomez, M. A.; Gomez-Herrero, J.; Jimenez, I. J Phys Chem B 2009, 113, 10104.
17. Sugama, T. Mater Lett 2006, 60, 2700.
18. Zou, H.; Xu, W.; Zhang, Q.; Fu, Q. J Appl Polym Sci 2006, 99, 1724.
19. Zhao, Y. F.; Xiao, M.; Wang, S. J.; Ge, X. C.; Meng, Y. Z. Compos Sci Technol 2007, 67, 2528.
20. Cho, M. Mater Trans 2008, 49, 2801.
21. Yang, J.; Xu, T.; Lu, A.; Zhang, Q.; Fu, Q. J Appl Polym Sci 2008, 109, 720.
22. Yu, S.; Wong, W. M.; Hu, X.; Juay, Y. K. J Appl Polym Sci 2009, 113, 3477.
23. Wu, D.; Wu, L.; Zhou, W.; Yang, T.; Zhang, M. Polym Eng Sci 2009, 49, 1727.
24. Yang, J.; Xu, T.; Lu, A.; Zhang, Q.; Tan, H.; Fu, Q. Compos Sci Technol 2009, 69, 147.
25. Lopez, L. C.; Wilkes, G. L. Polym-Plast Technol 1989, 29, 83.
26. Mark, J. E. Polymer Data Handbook; Oxford University Press: New York, 1999.
27. Morcom, M.; Atkinson, K.; Simon, G. P. Polymer 2010, 51, 3540.
28. Thostenson, E. T.; Chou, T.-W. J Phys D: Appl 2003, 36, 573.
29. Cadek, M.; Coleman, J. N.; Barron, V.; Hedicke, K.; Blau, W. J Appl Phys Lett 2002, 81, 5123.
30. Cebe, P. Polym Polym Compos 1995, 3, 239.
31. Byrne, M. T.; Gun'ko, Y. K. Adv Mater (Deerfield Beach, Fla) 2010, 22, 1672.
32. Hussain, F.; Hojjati, M.; Okamoto, M.; Gorga, R. E. J Compos Mater 2006, 40, 1511.
33. Spitalsky, Z.; Tasis, D.; Papagelis, K.; Galiotis, C. Prog Polym Sci 2010, 35, 357.
34. Rong, C.; Ma, G.; Zhang, S.; Song, L.; Chen, Z.; Wang, G.; Ajayan, P. M. Compos Sci Technol 2010, 70, 380.
35. Halpin, J. C.; Kardos, J. L. Polym Eng Sci 1976, 16, 344.
36. Available at: www.ticona.com Fortron PPS Datasheet.
37. Bangarusampath, D. S.; Ruckdaschel, H.; Altstadt, V.; Sandler, J. K. W.; Garray, D.; Shaffer, M. S. P. Polymer 2009, 50, 5803.
38. Li, L.; Li, C.; Ni, C.; Rong, L.; Hsiao, B. Polymer 2007, 48, 3452.
39. Díez-Pascual, A. M.; Naffakh, M.; Gómez, M. A.; Marco, C.; Ellis, G.; Martínez, M. T.; Ansón, A.; González-Domínguez, J. M.; Martínez-Rubi, Y.; Simard, B. Carbon 2009, 47, 3079.
40. Assouline, E.; Lustiger, A.; Barber, A. H.; Cooper, C. A.; Klein, E.; Wachtel, E.; Wagner, H. D. J Polym Sci Pol Phys 2002, 41, 520.
41. Bhattacharyya, A. R.; Sreekumar, T. V.; Liu, T.; Kumar, S.; Ericson, L. M.; Hauge, R. H.; Smalley, R. E. Polymer 2003, 44, 2373.
42. Haggenmueller, R.; Fischer, J. E.; Winey, K. I. Macromolecules 2006, 39, 2964.
43. Xu, D.; Wang, Z. Polymer 2008, 49, 330.